available at www.sciencedirect.com

ScienceDirect

journal homepage: www.elsevier.com/locate/biochempharm

Ca^{2+} extrusion in aged smooth muscle cells

Pedro J. Gomez-Pinilla [a], *Maria J. Pozo* [a], *Akemishi Baba* [b], *Toshio Matsuda* [b], *Pedro J. Camello* [a,*]

[a] *Department of Physiology, University of Extremadura, Campus Universitario, Fac Veterinary, 10071 Caceres, Spain*
[b] *Graduate School of Pharmaceutical Sciences, Osaka University, Japan*

ARTICLE INFO

Article history:
Received 11 May 2007
Accepted 25 June 2007

Keywords:
Calcium signals
Smooth muscle
PMCA
NCX
SERCA
Guinea pig

ABSTRACT

We investigated the effects of aging in Ca^{2+} extrusion mechanisms in smooth muscle bladder cells from 4 and 20–24-month-old guinea pigs using fluorescence microscopy and fura-2. Cells were challenged with a pulse of KCl immediately before perfusion with a Ca^{2+} free solution containing no inhibitors (control, untreated cells) or inhibitors of plasma membrane Ca^{2+} pump (PMCA, 1 mM La^{3+}), Na^+/Ca^{2+} exchanger (NCX, 1 μM SEA0400) or the sarcoendoplasmic Ca^{2+} pump (SERCA, 1 μM thapsigargin). Treatment of young adult cells with the inhibitors allowed estimating a relative contribution of 55% for NCX, 27% for PMCA and 31% for SERCA. Combination of two inhibitors at the same time showed the presence of interaction between extrusion mechanisms. In aged cells the $[Ca^{2+}]_i$ extrusion was impaired due to decrease of PMCA activity, as revealed by the loss of effect of La^{3+}, and to inhibitory interactions between NCX and SERCA activities, indicated by acceleration of decay in response to their respective inhibitors. In conclusion, in smooth muscle cells aging decreases the overall Ca^{2+} extrusion activity and modifies the interactions between the activities of the main Ca^{2+} removing mechanisms.

1. Introduction

Numerous stimuli and conditions operate cellular responses through changes in cytosolic Ca^{2+} concentration ($[Ca^{2+}]_i$) termed Ca^{2+} signals. These signals in turn regulate multiple cellular functions, such as contraction, secretion or gene regulation. The presence of age-related changes leads to the proposal of a "Ca^{2+} theory of aging" [1]. $[Ca^{2+}]_i$ signals are shaped by cytosolic Ca^{2+} binding capacity and Ca^{2+} transport mechanisms. $[Ca^{2+}]_i$ increases are due to Ca^{2+} influx from extracellular medium and release from internal stores (mainly sarcoendoplasmic reticulum). Subsequent recovery of $[Ca^{2+}]_i$ to basal levels is achieved by active transport either to the external medium, via plasma membrane Ca^{2+} pumps (PMCA) and Na^+/Ca^{2+} exchange (NCX), or into subcellular stores through sarcoendoplasmic reticulum Ca^{2+} (SERCA) pumps. The relative importance of these systems depends on both the type and status of the cell [2].

The effects of aging in Ca^{2+} homeostatic parameters have been studied mainly in excitable cells (for reviews see Refs. [3,4]). Thus, aged neurones display impairment of mechanisms such as Ca^{2+} buffering and Ca^{2+} extrusion [5–8], expression [9] and operation [10] of sarcoplasmic Ca^{2+} release channels, and refilling of intracellular neural pools [11,12]. In cardiac cells, aging increases the frequency of spontaneous localized Ca^{2+} release events (sparks) [13], and reduces depolarization-evoked $[Ca^{2+}]_i$ responses [13,14], while skeletal muscle SERCA and brain PMCA activities are impaired by age-related redox modifications [15].

Reports on smooth muscle Ca^{2+} signals during aging are scant. Arterial myocites show age-induced alterations in Ca^{2+} release through ryanodine and IP_3 receptors [16,17] and

* *Corresponding author*. Tel.: +34 927 257100; fax: +34 927 257110.
E-mail address: pcamello@unex.es (P.J. Camello).
0006-2952/$ – see front matter
doi:10.1016/j.bcp.2007.06.037

impaired SERCA function [18], while intestinal smooth muscle cells from aged rats show increases in both Ca^{2+} release from intracellular stores [19] and Ca^{2+} entry [20]. It has also been reported that aged arterial muscle shows increased $[Ca^{2+}]_i$ [17] and proliferation rate [21]. To our knowledge, there is no additional information in other smooth muscle types with the exception of changes in sensitivity to Ca^{2+} blockers in bladder muscle strips [22] and our recent description of impairment of Ca^{2+} influx in aged gallbladder smooth muscle [23]. These changes are likely to be related to age-related functional changes of smooth muscle, such as loss of gallbladder contraction [23,24] or impaired arterial tone and shift to hypertension [18,25].

Bladder smooth muscle shows alterations in contractility during aging ([26]; Gomez-Pinilla, Camello and Pozo, unpublished observations), and some of them have been postulated to be related to changes in Ca^{2+} homeostasis [22]. Ca^{2+} extrusion systems are main determinants in bladder contraction [27]. Therefore, in the present study we have studied the possible modification of smooth muscle Ca^{2+} clearance mechanisms by aging.

2. Methods

2.1. Cell isolation

Single cells from detrusor smooth muscle of young adults (4-month-old) or aged guinea pigs (20–24-month-old) were obtained by enzymatic digestion. After anaesthesia and cervical dislocation, urinary bladder was removed, placed in a sylgard plate filled of Krebs-Henseleit solution (K-HS, see Section 2.3), trimmed free of fatty tissue and opened along its longitudinal axis. Later the bladder was pinned to the sylgard plate and the urothelium was removed carefully. Subsequently, about 20 mg of urinary bladder muscle was cut into small pieces and incubated during 35 min at 37 °C in enzyme solution (ES, for composition see Section 2.3) supplemented with 1 mg/ml BSA, 1 mg/ml papain, and 1 mg/ml dithioerythritol. The tissue was then transferred to fresh ES containing 1 mg/ml BSA, 1 mg/ml collagenase, and 100 μM $CaCl_2$ and incubated for 10 min at 37 °C. The tissue was then washed three times using ES, and the single smooth muscle cells were isolated by several passages of the tissue pieces through the tip of a fire-polished pipette. The resultant cell suspension was kept in ES at 4 °C until use, generally within 6 h. Both cell viability (assayed by fast trypan blue staining) and cell length was similar in young and adult cells (adult: 52.02 ± 1.48 μm; aged: 47.35 ± 2.52 μm). Experiments were performed at room temperature.

2.2. Cell loading and $[Ca^{2+}]_i$ determination

$[Ca^{2+}]_i$ was determined by epifluorescence microscopy using the fluorescent ratiometric Ca^{2+} indicator fura-2. Isolated cells were loaded with 4 μM fura-2-AM at room temperature for 25 min. An aliquot of cell suspension was placed in an experimental chamber made with a glass poly-D-lysine treated coverslip (0.17 mm thick) filled with Na^+-HEPES solution (for composition see Section 2.3) and mounted on the stage of an inverted microscope (Diaphot T2000; Nikon). After cell sedimentation, a gravity-fed system was used to perfuse the chamber with Na^+-HEPES solution in the absence or presence of experimental agents. For deesterification of the dye, >20 min were allowed to elapse before Ca^{2+} measurements were started. Cells were illuminated at 340 and 380 nm by a computer-controlled monochromator (Optoscan, Cairn Research) at 0.3 Hz, and the emitted fluorescence was selected by a 500-nm long-pass filter. The emitted images were captured with a cooled digital charge-coupled device camera (ORCAII-ER; Hamamatsu Photonics) and recorded using dedicated software (Metafluor, Universal Imaging). The ratio of fluorescence at 340 nm to fluorescence at 380 nm (F_{340}/F_{380}) was calculated pixel by pixel and used to indicate the changes in $[Ca^{2+}]_i$. For the purpose of the present study calibration of ratio values was not necessary due to the normalization procedure (see below).

2.3. Solutions and drugs

The K-HS contained (in mM): 113 NaCl, 4.7 KCl, 2.5 $CaCl_2$, 1.2 KH_2PO_4, 1.2 $MgSO_4$, 25 $NaHCO_3$, and 11.5 D-glucose. This solution had a final pH of 7.35 after equilibration with 95% O_2–5% CO_2. The ES used to disperse cells was made up of (in mM): 10 HEPES, 55 NaCl, 5.6 KCl, 80 sodium glutamate, 2 $MgCl_2$, and 10 D-glucose, with pH adjusted to 7.3 with NaOH. The Na^+-HEPES solution contained (in mM): 10 HEPES, 140 NaCl, 4.7 KCl, 2 $CaCl_2$, 2 $MgCl_2$, and 10 D-glucose, with pH adjusted to 7.3 with NaOH. The Ca^{2+}-free Na^+-HEPES solution was prepared by substituting EGTA (1 mM) for $CaCl_2$. Drug concentrations are expressed as final bath concentrations of active species. Drugs and chemicals were obtained from the following sources: 1,4-dithio-D,L-threitol, La^{3+} and thapsigargin were from Sigma Chemical (St. Louis, MO); fura-2-AM was from Molecular Probes (Molecular Probes Europe, Leiden, Netherlands); collagenase was from Fluka (Madrid, Spain); and papain was from Worthington Biochemical (Lakewood, NJ). SEA0400 (2-[4-[(2,5-difluorophenyl)methoxy]phenoxy]-5-ethoxyaniline) was synthesized in Taisho Pharmaceutical Co., Ltd. (Saitama, Japan). Other chemicals used were of analytical grade from Panreac (Barcelona, Spain). Stock solutions of fura-2-AM and thapsigargin were prepared in DMSO. The solutions were diluted such that the final concentrations of DMSO were ≤1% (v/v), which do not interfere with fura-2 fluorescence.

2.4. Data processing and statistics

To analyze $[Ca^{2+}]_i$ clearance the ratio traces were clipped from the start of the decay and averaged across different experiments for presentation purposes and to fit exponential decay equations (see below). When comparing between different experimental conditions, the raw data were previously normalized following the formula

$$\text{Normalized}_i = \frac{\text{raw}_i - \text{raw}_{\text{previous}}}{\text{raw}_{\text{start}} - \text{raw}_{\text{previous}}},$$

where $\text{raw}_{\text{start}}$ and $\text{raw}_{\text{previous}}$ are respectively the original ratio values at the beginning of the decay and before stimulation with KCl. This procedure allows direct comparison of the

speed and the extent of $[Ca^{2+}]_i$ recovery to resting levels independently of possible differences in peak and/or resting ratio or calibrated $[Ca^{2+}]_i$ values, which poses uncertainties in the interpretation of the decays.

The average decay (either raw or normalized) was fitted with a two phase exponential decay

$$y = \text{Plateau} + \text{Span1} \times \exp(-k1 \times x) + \text{Span2} \times \exp(-k2 \times x)$$

where y and x are ratio and time (s), Plateau, Span1 and Span2 are the ratio at the end of the decay and the initial and second amplitude associated to each exponential component, and $K1$ and $K2$ (s^{-1}) are the rate constants of the first and second exponential components. The fitting procedure was constrained to Plateau levels $\geq$90% of the value measured at the end of the recorded decay. Correlation was always higher than 90%. Fitting with a single phase exponential decay gave always a lower correlation.

To evaluate and visualize the contribution of different mechanisms in the removal of Ca^{2+} clearance graphs ($d[Ca^{2+}]_i/dt$ versus $[Ca^{2+}]_i$) we followed a procedure previously described [28]: (1) after fitted with the two phase exponential described above, the fitted line was derived (dRatio/dt) and then plotted versus the ratio values obtained from the exponential fit; (2) the clearance plots of comparable experimental groups (control versus treated, young versus aged) were graphed together and fitted with a fourth order polynomial equation. For clarity, only the fitted polynomial fit was graphed in most of the figures. To visualize the component associated to an extrusion mechanism, the plot obtained in presence of an inhibitor was subtracted from the plot from untreated cells.

To perform statistical comparison of the rate of decay of different conditions, the time to reach 50% of the initial ratio ($t_{1/2}$) was calculated for each individual cell and subsequently averaged. The same procedure was followed for the plateau attained at the end of the decay (final recovery). With the exception of the initial comparison between young and aged cells, we did not compare the rate constants and plateaus generated by the second order exponential fit described above because it would complicate the description of the results without adding further information respect to this simplest procedure. Estimation of the contribution of each homeostatic mechanism was performed following the procedure developed by Paul and co-workers [27], calculating the percentage decrease in the average $t_{1/2}$ induced by the inhibitor of the desired mechanism (see Section 3) using the average of the untreated group (either adult or aged) as control (100%).

Statistical differences between two means were determined by Student's t-test, and two-way Anova was used to determine interaction of age and treatment. Differences were considered significant at $P < 0.05$. Mean values are presented as average ± S.E.M.

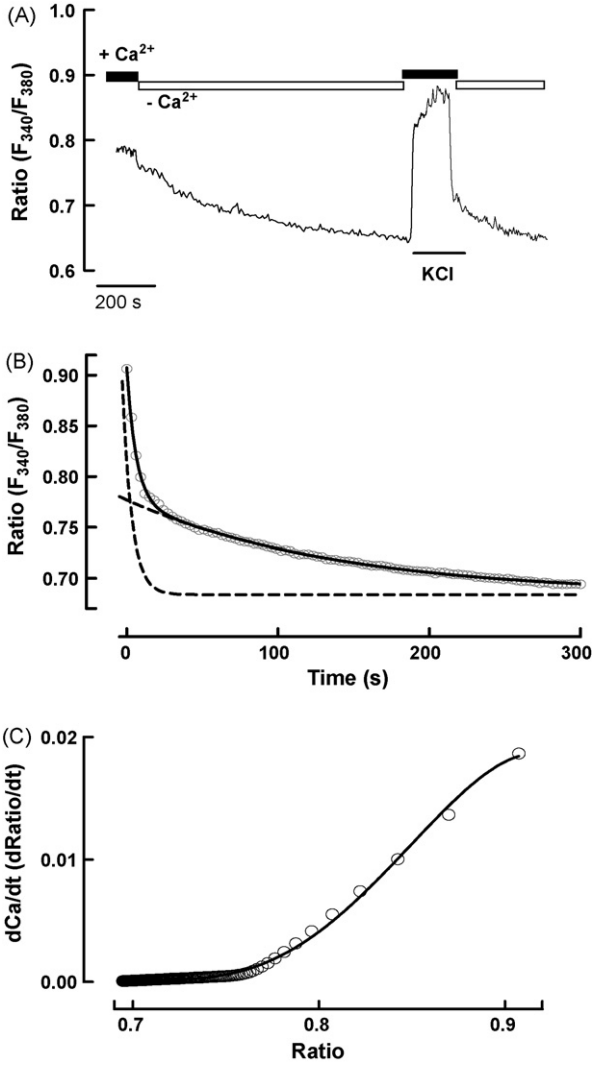

Fig. 1 – $[Ca^{2+}]_i$ decay after KCl-evoked depolarization in urinary bladder smooth muscle cells. (A) Original recording of fura-2 ratio of fluorescence of a single bladder muscle cell showing the protocol used to study Ca^{2+} clearance. Cells were stimulated with a pulse of 60 mM KCl solution and then they were perfused with a Ca^{2+} free solution (1 mM EGTA) in absence (control) or presence (not shown) of Ca^{2+} transport inhibitors. For thapsigargin or SEA0400 cells were pretreated for 10 min in Ca^{2+} free solution (no drugs addition in control cells). (B) Averaged record of Ca^{2+} decay from untreated young bladder cells, showing actual data (symbols) and a fitted two phase exponential decay function (solid line). The two dashed lines correspond to the two exponential components of the function. (C) Clearance plot obtained from data in panel B by time derivation of the fitted equation ($d[Ca^{2+}]_i/dt$) and subsequent plot against $[Ca^{2+}]_i$ (ratio). The line corresponds to a fourth order polynomial function.

3. Results

To study Ca^{2+} extrusion we followed the protocol shown in Fig. 1. Bladder smooth muscle cells were stimulated with a K^+-rich depolarizing solution (60 mM KCl) until a steady-state was achieved, and then were perfused with a Ca^{2+}-free solution to decrease $[Ca^{2+}]_i$ level. Previous to KCl application, cells were perfused for 10 min with a Ca^{2+}-free medium in absence (control, untreated cells) or presence of Ca^{2+} transport

inhibitors (SEA0400- or thapsigargin-treated cells), which were also present during KCl application and the subsequent decay. These inhibitors (and the corresponding perfusion period in the control group) were applied in absence of extracellular Ca^{2+} to avoid premature and de-regulated Ca^{2+} increases due to activation of capacitative Ca^{2+} entry (thapsigargin) or to blockade of NCX activity (SEA0400). As observed, removal of KCl-induced a decay in $[Ca^{2+}]_i$, which approached to resting levels within 300 s. The kinetic of this decay was used as an index of Ca^{2+} extrusion mechanisms. The $[Ca^{2+}]_i$ profile was fitted with a two phase exponential decay (Fig. 1B), which was used to build clearance plots (dRatio/dt versus Ratio, see Section 2) (Fig. 1C), in order to visualize the speed of the Ca^{2+} decay along the recovery process (from stimulated to resting $[Ca^{2+}]_i$). This observed pattern, with an early fast decay followed by a slower phase, is suggestive of at least two components or mechanisms in the Ca^{2+} clearance process [28].

Fig. 2A shows the average raw $[Ca^{2+}]_i$ decay for young adult and aged bladder smooth muscle cells. The resting ratio value immediately before KCl application, corresponding to basal $[Ca^{2+}]_i$ for non-stimulated cells in Ca^{2+}-free medium, was slightly higher in old cells (0.6947 ± 0.014 F_{340}/F_{380}, $n = 63$ cells, eight experiments) than in young adult cells (0.6919 ± 0.011 F_{340}/F_{380}, $n = 92$ cells, eight experiments), as it was the ratio value for the KCl-induced $[Ca^{2+}]_i$ increase at the initiation of the decay (young adult 0.9065 ± 0.0175 F_{340}/F_{380}, old 0.9145 ± 0.0202 F_{340}/F_{380}). The extrusion was apparently slowed in aged cells, as indicated by the increase in the decay half-time ($t_{1/2}$) from 14.357 ± 1.405 s (young adult cells, $n = 92$ cells, eight experiments) to 42.008 ± 6.448 s (aged cells, $n = 63$ cells, eight experiments). This is further supported by the age-induced reduction in the initial rate constant (see Fig. 2C, young: 0.1617 ± 0.0034 s^{-1}; old: 0.0764 ± 0.0022 s^{-1}, $P < 0.0001$).

At the end of the studied period aged cells showed a decreased recovery (Fig. 2A), which resulted in a shorter second span for the fitted exponential function (young adult: 0.0931 ± 0.0007 F_{340}/F_{380}, aged: 0.1117 ± 0.001 F_{340}/F_{380}, $P < 0.0001$) and the consequent increase in the final plateau (Fig. 2C, young adult 0.6838 ± 0.0009 F_{340}/F_{380}, old 0.7107 ± 0.0007, F_{340}/F_{380}, $P < 0.0001$). This result induced a false acceleration of the second phase of the decay, as indicated by the increase in the second rate constant (from 0.0072 ± 0.0002 to 0.0087 ± 0.0002 s^{-1}, $P < 0.0001$) (Fig. 2C) although at that level the decay was parallel for young and old cells (Fig. 2A). Therefore, the simplest and straightforward comparison of the observed $t_{1/2}$ and final plateau is as effective as the fitting of exponential decays to estimate quantitatively the decay activity and it was used for the rest of the study.

Though the difference of the $[Ca^{2+}]_i$ decay between young and old cells was readily apparent using averaged raw ratios, we also compared the decays using mean of normalized ratios (Fig. 2B), since it avoids uncertainties due to differences in the absolute ratio values (see Section 2) and allows an immediate evaluation of the rate and the extent of the recovery. Fig. 2C shows that first rate constant calculated from normalized values was again significantly higher in control cells, while the fitted final plateau was also higher in aged cells (young adult -0.0897 ± 0.0059; $n = 92$, old 0.0521 ± 0.0137, $n = 63$, $P < 0.001$). In this case the difference in the observed plateau at the end of the recovery was also statistically significant (young adult -0.0276 ± 0.0189, normalized ratio; $n = 92$, old 0.0873 ± 0.0288, $n = 63$, $P < 0.001$).

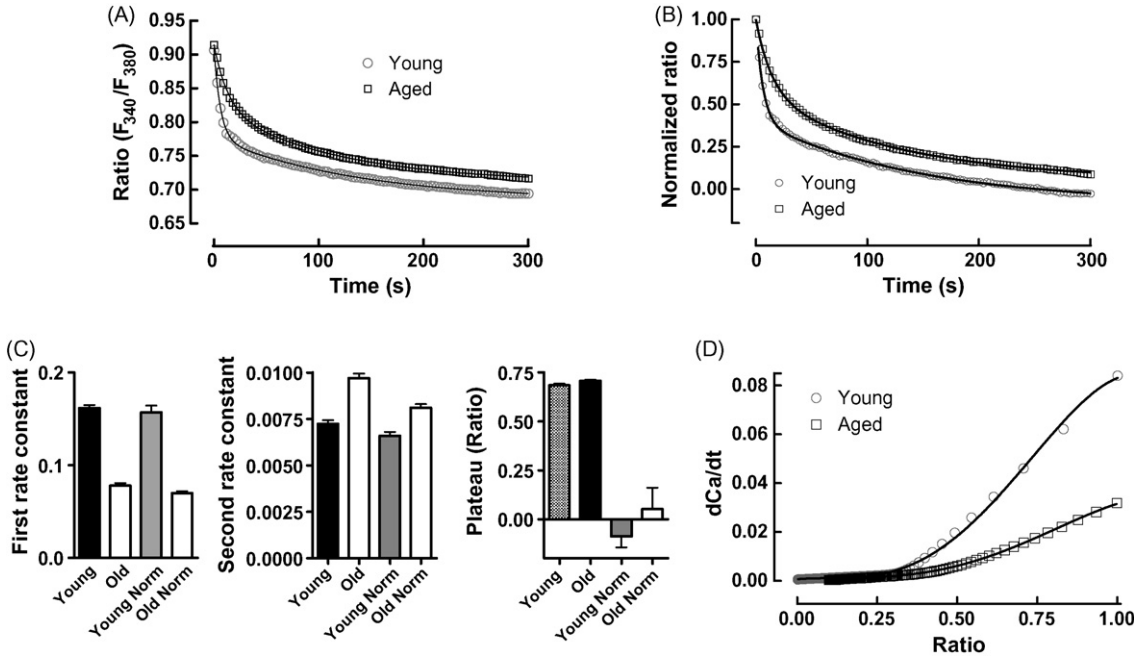

Fig. 2 – Effect of aging in Ca^{2+} clearance activity. (A and B) Average $[Ca^{2+}]_i$ decay after a KCl depolarizing pulse in young and aged smooth muscle cells. For the sake of clarity error bars are not shown. The solid lines correspond to two phase exponential decay functions fitted to observed raw (A) or normalized (B) fura-2 ratio. (C) First and second rate constants (s^{-1}) and final plateau ratio for the fitted exponential decays of panels A and B. (D) Clearance plots for normalized extrusion decays in young and aged cells. Data from eight experiments.

Irrespective of small differences between absolute values for the initial phase of the $[Ca^{2+}]_i$ decay, clearance operates at a significantly impaired rate in senescent cells for most of the $[Ca^{2+}]_i$ range, as inferred by comparing the clearance plots of aged and young adult bladder cells (Fig. 2D), which shows a substantial loss of clearance activity in aged cells (more than 50%).

Ca^{2+} extrusion from cytosol is operated by three main transport mechanisms: PMCA pumps of the plasma membrane, Na^+/Ca^{2+} exchange with extracellular medium and SERCA pumps of the sarcoplasmic reticulum. To test the contribution of these mechanisms in young and aged cells, we used specific inhibitors: 1 μM SEA0400 for NCX, 1 mM La^{3+} for PMCA and 1 μM thapsigargin for SERCA pumps. The relative importance of these systems in young and aged cells was estimated through the effects of the inhibitors on the clearance plots and on the $t_{1/2}$ and final recovery values measured in each condition.

Treatment of young adult cells with La^{3+} slowed the initial part of the decay, which showed a higher $t_{1/2}$ ($P < 0.05$, *t*-test) (Fig. 3D), and examination of the clearance plots showed a clear retard in the initial phase of the decay, when the fractional decay is above 50% of the initial ratio value (Fig. 3A), indicating the contribution of PMCA to this phase of the extrusion. This was further confirmed by a decrease in the first rate constant ($0.1815 \pm 0.0008\ s^{-1}$ versus $0.0955 \pm 0.0005\ s^{-1}$, control and La^{3+}, respectively, $P < 0.0001$, *t*-test). However, La^{3+} did not change the observed final plateau (control: -0.0276 ± 0.0189, $n = 92$ cells, eight experiments, La^{3+} -0.0257 ± 0.0214, $n = 59$ cells, six experiments, not significant). By the contrary, when aged cells were perfused with La^{3+} the initial rate of the decay did not decrease, as it can be observed in Fig. 3A and D. The first rate constant and the $t_{1/2}$ values were not significantly different between untreated and treated aged cells. By the contrary, the total recovery was impaired in La^{3+}-treated aged cells, as indicated by the plateau values (0.0873 ± 0.0288, $n = 63$ cells, eight experiments, versus 0.1769 ± 0.0339, $n = 61$ cells, eight experiments, control and treated cells respectively, $P < 0.05$). These results indicate that, in aged cells PMCA activity has a low contribution on Ca^{2+} extrusion at high $[Ca^{2+}]_i$ levels but increases its role for near-resting values.

Treatment of young cells with SEA0400 to inhibit NCX activity resulted in a clear inhibition of the rate of decay at high and also at moderate $[Ca^{2+}]_i$ levels, when the fractional recovery was even lower than 50%, as shown by the clearance plots shown in Fig. 3B. Although SEA0400 did not change the fitted rate constants of the decay, it enhanced $t_{1/2}$ significantly (Fig. 3D). The drug also increased the final normalized plateau from -0.0276 ± 0.0189 ($n = 92$) to 0.1159 ± 0.0447 ($n = 36$ cells, three experiments, $P < 0.005$, *t*-test). In aged cells, application of SEA0400 also reduced the final recovery (untreated 0.0873 ± 0.0288, $n = 63$, treated cells 0.2340 ± 0.0439, $n = 12$ cells, five experiments, $P < 0.05$), and induced a small and not significant decrease in the observed half-life (Fig. 3D). This effect is in keeping with the loss of sensitivity to SEA0400 at high $[Ca^{2+}]_i$ levels revealed by the clearance plots, which show even a slight increase in speed above 50% fractional recovery (Fig. 3B).

Thapsigargin, a specific inhibitor of the sarcoplasmic reticulum SERCA pumps, did not change the measured final recovery (untreated young cells -0.0276 ± 0.0189, $n = 92$,

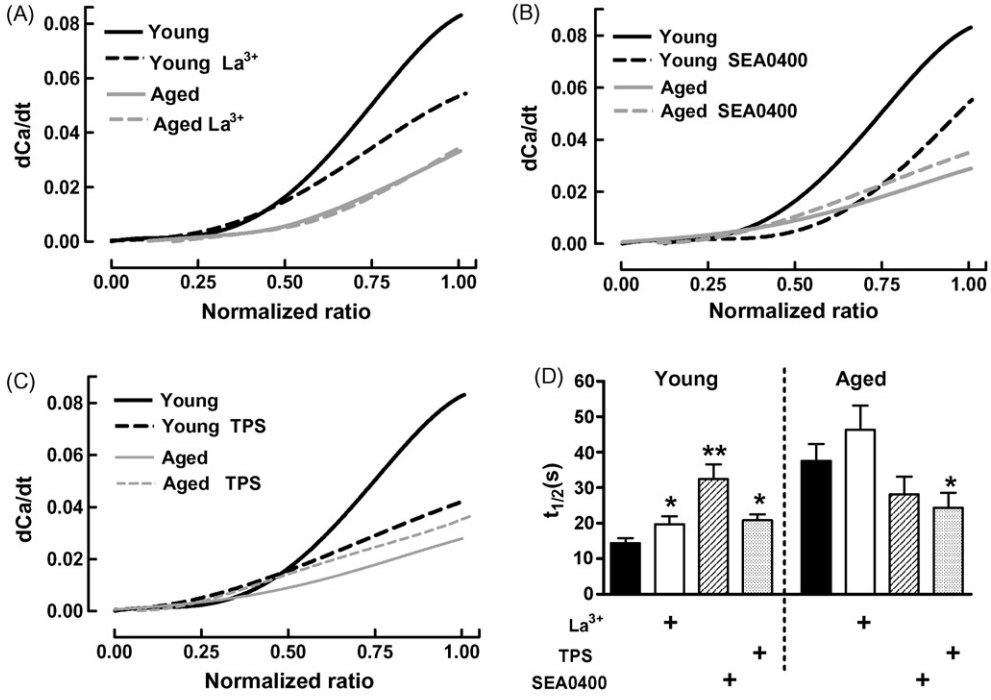

Fig. 3 – Effects of inhibitors of PMCA, NCX and SERCA on the rate of Ca^{2+} clearance in young and aged cells. Clearance plots in the absence (solid lines) or the presence (dashed lines) of 1 mM La3+ (A) to block PMCA activity, 1 μM SEA0400 (B) to inhibit NCX exchange or 1 μM TPS (C) to block SERCA activity. (D) Average (±S.E.M.) $t_{1/2}$ for each experimental condition. Two-way Anova test showed significant effect of age ($P < 0.002$) and significant interaction with treatment ($P < 0.01$). $^{*}P < 0.05$, $^{**}P < 0.01$ respect untreated cells. Data from three to eight experiments.

thapsigargin-treated -0.0680 ± 0.0358, $n = 35$ cells, three experiments, normalized ratio, not significant, *t*-test). However, TPS retarded the initial part of the extrusion, as shown by the initial phase of the clearance plot (normalized ratios > 0.5) (Fig. 3C) and by an increased $t_{1/2}$ ($P < 0.005$, *t*-test) (Fig. 3D). In aged cells the effects of thapsigargin were clearly different. The drug induced a slight increase in the final plateau at the limit of statistical significance (control 0.0873 ± 0.0288, $n = 63$, TPS 0.2022 ± 0.0562, $n = 14$ cells, three experiments, $P < 0.05$, one-tailed *t*-test), but decreased the clearance half-life (Fig. 3D). Examination of the clearance plot (Fig. 3C) reveals that in TPS-treated aged cells the initial speed of the recovery is higher than in untreated cells, dropping slightly below the later when $[Ca^{2+}]_i$ approaches to resting values, a behaviour opposite to that displayed by young cells (Fig. 3C). This suggests that that aging changes the role of SERCA activity in Ca^{2+} clearance.

The previous results indicate that the most important mechanism to decrease $[Ca^{2+}]_i$ in young adult bladder smooth muscle is the NCX exchanger (SEA0400 sensitive), with PMCA (La^{3+} sensitive) and SERCA-operated pools (TPS sensitive) operating when intracellular Ca^{2+} is high or moderately high. In senescent cells the apparent conclusion is that none of these mechanisms are responsible for Ca^{2+} clearance, given that the inhibitors did not impair the extrusion (or even enhanced it) (for an estimation of the relative contributions see Section 2 and Table 1). To confirm the effects of inhibiting extrusion mechanisms, we applied simultaneously inhibitors for two of the transport routes. Under this condition, the remaining activity is due to the third route (or to alternative Ca^{2+} transport systems). The corresponding clearance plots are shown in Fig. 4. The combination of TPS plus La^{3+} in young cells induced a retard higher than that attained by either TPS or La^{3+} alone, as indicated by the increased $t_{1/2}$ and by comparison of the clearance plots (see Figs. 3 and 4). In addition, the average normalized plateau at the end of the recorded period (0.1018 ± 0.0348, $n = 43$ cells, four experiments) was higher than that obtained by each compound alone (La^{3+}: -0.0257 ± 0.0214; TPS: 0.0680 ± 0.0358). By the contrary, this pattern of inhibition was absent in aged cells: the final plateau was even lower in treated (0.0413 ± 0.0283, $n = 22$ cells, four experiments) than in untreated aged cells (0.0873 ± 0.0288, $n = 63$), and the clearance plots show a clear acceleration of the decay, also indicated by a reduced $t_{1/2}$ (Figs. 3 and 4).

The same approach was used to isolate the other components of extrusion activity. To isolate SERCA reuptake we inhibited Ca^{2+} extrusion through plasma membrane by combining La^{3+} and SEA0400. This treatment increased the observed final plateau in young adult cells from -0.0276 ± 0.0189 to 0.0378 ± 0.034 ($n = 53$ cells, five experiments), and in aged cells from 0.0873 ± 0.0288 ($n = 63$) to 0.1219 ± 0.0285 ($n = 53$ cells, seven experiments). However, the effect of SEA0400 plus La^{3+} on the rate of decay, as judged by the clearance plots (Fig. 4B), was totally residual in old cells while in young adult cells there was a clear retard for high and intermediate $[Ca^{2+}]_i$ levels.

To dissect contribution of PMCA to Ca^{2+} decay, we perfused smooth muscle cells with a combination of TPS and SEA0400. In young adult cells this treatment induced a retard of the rate at the beginning of the decay, above 50% of the recovery, while the rate of the second half of the recovery was close to that in untreated cells (Fig. 4C). In fact, the normalized final plateau in treated cells (-0.0336 ± 0.0396, $n = 34$ cells, four experiments) showed no significant difference respect control cells (-0.0276 ± 0.0189, $n = 92$). By the contrary, in cells from aged animals there was no inhibition, showing a shortened half-life (Fig. 4D) and an accelerated rate of decay from high to resting $[Ca^{2+}]_i$ levels (Fig. 4C), when treated cells decline slightly slower than untreated cells.

To estimate the age-related changes of each Ca^{2+} removal system in our experimental conditions we followed the method described by Paul and co-workers [27]: the overall rate constant of the decay, estimated as the inverse of observed half-life values ($t_{1/2}^{-1}$ or τ_{Total}), can be considered to be the sum of three main components: $\tau_T = \tau_{PMCA} + \tau_{SEA} + \tau_{SERCA}$. The contribution of each component was calculated as $i = (1 - \tau_X/\tau_{CONTROL}) \times 100$, i.e. the percentage decrease in the rate constant in response to a treatment. Table 1 shows relative contributions of each system in young adult and in aged cells. In adult cells the main contributor is NCX (more than 50%), with contribution for PMCA and SERCA around 30%. The sum of the three components (114%) is higher than 100%, suggesting some kind of interaction between one another. We also calculated the contribution for two systems at a time, corresponding to the effect of the combination of two inhibitors. The sum of this value plus the contribution of the third system should approach 100; for example, contribution of SERCA (31.04, TPS) plus contribution of NCX and PMCA (57.25, SEA0400 + La^{3+}) amounts 88.03%. The most striking feature is the low apparent contribution for combined SERCA and NCX (only 11.58%, TPS + SEA0400, far from the expected 73%). Therefore, PMCA activity is somehow inhibited or disguised by NCX and SERCA, so that when activities of NCX and SERCA are intact La^{3+} treatment induces a 27% decrease, while the application of SEA0400 plus TPS decreases the rate only by 11% because PMCA is no longer inhibited and its contribution is increased (~88%). Although to a much lesser extent, a similar situation was found for SERCA: its

Table 1 – Estimation of the relative contribution of PMCA, NCX and SERCA to $[Ca^{2+}]_i$ decays in bladder smooth muscle cells

Inhibitor	La^{3+}	SEA0400	TPS	TPS + SEA0400	TPS + La^{3+}	SEA0400 + La^{3+}
Young	27.29	55.75	31.04	11.58	61.64	57.25
Aged	9.33	−35.87	−72.41	−45.29	−140.96	−39.23
Extrusion activity	−PMCA	−NCX	−SERCA	PMCA	NCX	SERCA

Contribution for each Ca^{2+} removing mechanism was calculated using inverse of $t_{1/2}$ (τ_i) following the formula $((1 - \tau_i^{-1}/\tau_{Total}^{-1}) \times 100)$. Negative values indicate that the treatment *accelerated* the decay rate.

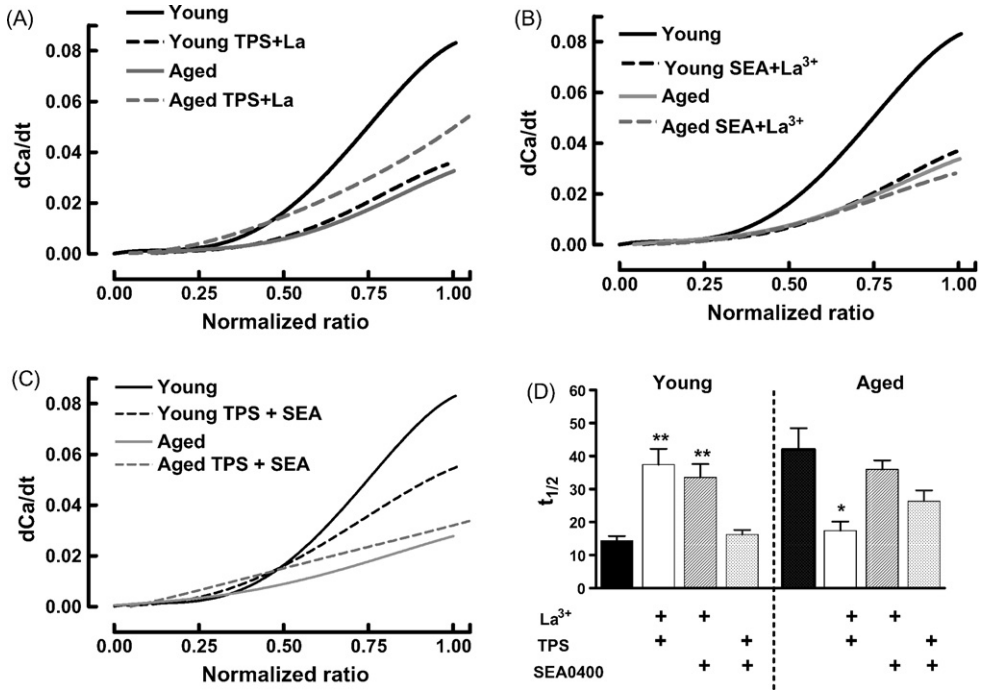

Fig. 4 – Effects of combined inhibition of PMCA, NCX and SERCA on the rate of clearance in young and aged bladder smooth muscle cells. Cells were treated with a combination of inhibitors of two of the three main Ca^{2+} removing mechanisms to isolate the clearance activity of NCX (A, TPS plus La^{3+}), SERCA (B, SEA0400 plus La^{3+}) or PMCA (C, TPS plus SEA0400) (dashed lines). Clearance plots for untreated cells are also shown (solid lines). Panel D shows the mean ± S.E.M. of the measured $t_{1/2}$ for each experimental condition. Two-way Anova showed interaction of age with treatment ($P < 0.001$). $^{*}P < 0.01$, $^{**}P < 0.001$ respect untreated cells. Data from four to eight experiments.

contribution is slightly increased from 31% (TPS treatment, with NCX and PMCA operative) to 43% for SEA0400 and La^{3+} treatment, indicating some inhibition by NCX and PMCA activity. By the contrary, in the case of NCX the estimated contribution was decreased by inhibition of PMCA and SERCA from 55% (SEA0400 alone) to 38% (100-62, La^{3+} + TPS), indicating that its role in Ca^{2+} extrusion is enhanced in presence of SERCA and PMCA pumps.

When this approach was used in aged cells, we obtained *negative* contribution in all conditions, except for La^{3+}-treated cells. These figures result from a trade-off between extrusion from the cytosol and inhibition of other Ca^{2+} transport systems, and are in keeping with the observed acceleration of the decay in response to inhibitors. Similar to adult young cells, the contribution of PMCA was also inhibited by NCX and SERCA (TPS plus SEA0400, which leave PMCA as the main route for extrusion, induced a clear acceleration of the decay), but was weaker than in young adult cells in La^{3+}-treated cells (less than 10%). SERCA apparently inhibits the other transport routes, given the strong increase on decay rate in response to TPS (72%). In the case of NCX, it seems also to inhibit the other transporters, but contrary to young cells, NCX was apparently inhibited by the other routes, since inhibition of SERCA and PMCA (TPS + La^{3+}) strongly enhanced the rate of decay. Therefore, the effect of aging is not a simple loss of sensitivity to the inhibitors (which should induce no effect instead of acceleration), but a complex set of interactions between the main Ca^{2+} extrusion systems.

4. Discussion

The present study shows that both the speed and the pharmacology of the Ca^{2+} extrusion mechanisms in smooth muscle are modified by aging. To our knowledge this is the first detailed account of how aging alters each of the main Ca^{2+} clearing systems.

Our results indicate that bladder smooth muscle cells remove Ca^{2+} from cytosol using the three ''classic'' transport systems, i.e. SERCA reuptake into stores, and NCX exchange and PMCA pumps located at the sarcolemma. The most active system is the NCX, as revealed by the effect of the specific inhibitor SEA0400 [29] on both the amplitude and the speed of the recovery. The dominance of this system seems to spread to both elevated and near-resting $[Ca^{2+}]_i$ levels, as judged by examination of the clearance plots, while inhibition of PMCA or SERCA seems less effective at low Ca^{2+} levels.

Our estimates of the contribution of each Ca^{2+} transport system (NCX 56%, PMCA 27% and SERCA 31%) are in line with recent reports about contractility of bladder muscle strips from normal and PMCA gene-ablated mice [27]. These authors also found that cooperation between the systems is not always additive, as indicated by our finding that combination of SEA0400 with either La^{3+} or TPS did not increase inhibition. Only when La^{3+} and TPS were combined there was addition between the relative contributions of PMCA and SERCA. Moreover, addition of the three contributions exceeded 100%, which also suggests the presence of interaction between

the transport systems. Therefore, our data reinforce the concept that in physiological conditions Ca^{2+} clearing mechanisms do not operate independently. This cooperation has been previously postulated to explain experimental data regarding contractility [27], electrophysiology [30,31] and $[Ca^{2+}]_i$ signals [32–34]. So, it has been proposed that spatial arrangements of transport systems can induce a vectorial movement of Ca^{2+} ions from SERCA-driven internal stores to plasma membrane transporters [33,34]. Following this, inhibition of two ''consecutive'' transporters would be redundant, therefore yielding less than additive effect. The physical basis for this mechanism is based not only in the ''superficial barrier'' theory [34,35] but in the presence of both NCX and PMCA in smooth muscle caveolae [36]. In fact, bladder smooth muscle cells show similar examples of tight apposition of different Ca^{2+} transport systems, such as clusters of channels in plasmalemmal caveolae which operate as a functional unit in $[Ca^{2+}]_i$ signals [37] and buffering of plasmalemmal Ca^{2+} current by SERCA pumps [38].

This study indicates that the mechanisms responsible for Ca^{2+} extrusion in urinary bladder smooth muscle are impaired in senescent cells. Thus, overall Ca^{2+} extrusion was inhibited in aging cells compared to young cells irrespective of the actual $[Ca^{2+}]_i$ level. In addition, inhibition of PMCA, NCX or SERCA, which impaired the rate of clearance in control cells, did not retard extrusion in senescent cells, with the exception of a minor inhibition of the final recovery. Therefore, our data indicate apparently that in aged cells the initial phase of the recovery is not driven by the three classic extrusion systems, which would regain importance when Ca^{2+} approaches basal levels. Mitochondrial uptake could serve as a compensatory extrusion mechanism because they accumulate Ca^{2+} upon $[Ca^{2+}]_i$ signals and release it later to the cytosol [39]. In fact, in some excitable cells mitochondrial Ca^{2+} uptake has been reported to compensate for age-related SERCA impairment [40]. However, other reports failed to find this effect [41], and senescent neurones show a progressive depolarization of the mitochondrial membrane [42], incompatible with a rapid Ca^{2+} uptake necessary to participate in the $[Ca^{2+}]_i$ decay pattern studied in our experiments. Moreover, aging depolarizes mitochondria of bladder muscle cells (Gomez-Pinilla, Camello and Pozo, manuscript in preparation), in keeping with age-related impairment of key metabolic enzymes of the mitochondria [43]. Given that mitochondrial membrane potential is the main factor driving Ca^{2+} uptake, these observations make highly unlikely the participation of mitochondria in the delayed recovery of aged cells, because aged mitochondria should accumulate a higher amount of Ca^{2+} during the sustained KCl response in order to release it into the cytosol during the decay phase.

A possibility to explain the apparent non-participation of the classical Ca^{2+} extrusion mechanisms in aged smooth muscle cells could be the existence of an inhibitory relationship among them, as will be discussed below, or changes in the sensitivity of these transporters to the normal inhibitors. In line with this, a striking observation is the enhanced extrusion rate in presence of thapsigargin or SEA0400 in aged cells, which also reveals that the transporters do participate in the extrusion (otherwise the inhibitors would be without effect). Several explanations could account for this result. First, SERCA inhibition could stimulate PMCA pumps situated in close apposition, a mechanism previously reported for thapsigargin-induced acceleration of Ca^{2+} decays [44]. Second, during the KCl pulse SERCA pumps could ''prime'' intracellular stores with a fast turnover, so that continuous leak from this pool would ''retard'' the posterior decay. A similar picture previously has been reported in pancreatic acinar cells [45]. Under this condition, if the Ca^{2+} release from this pool to the cytosol is faster than the reuptake activity, the net effect of SERCA inhibition would be an apparent acceleration of Ca^{2+} extrusion.

As for NCX, it has been shown in bladder myocites that this exchanger operates at a point close to equilibrium, so that slight changes in intracellular Na^+ concentration (amplitudes of less than 5 mM) can switch the exchange from forward (Ca^{2+} extrusion) to reverse mode, therefore serving as a route for Ca^{2+} influx [46]. If the depolarization created by KCl in old cells induces a persistent increase in cytosolic Na^+, NCX operating in reverse mode could retard the decay, so that SEA0400 inhibition would accelerate the Ca^{2+} recovery. Contrary to this possibility, however, is the low affinity of SEA0400 for the reverse mode of the exchanger [47]. Other possible mechanism for the altered pattern of NCX influence is chemical modifications of the transporter associated to aging. This protein shows activity changes in response to cysteine modification by sulfhydryl reagents [48], and SEA0400 effects can change by modifications of determinant residues [49]. It is known that other Ca^{2+} signalling proteins, such as calmodulin and SERCA, also undergo age-related oxidative modifications leading to inhibition [15], although more investigation is necessary to know whether this is the case for NCX.

The functional implications of our finding are diverse for a smooth muscle with phasic activity as is the case for the detrusor. A retarded clearance rate involves that with each $[Ca^{2+}]_i$ transient the exposure to raised Ca^{2+} levels is prolonged. Contractility of urinary bladder muscle is controlled by spontaneous action potentials and several Ca^{2+}-activated K^+ channels of the plasma membrane (reviewed by [50]), so that a decreased rate of Ca^{2+} clearance in aged animals would likely lead to a depressed contractility, in line with our finding using the same model (manuscript in preparation).

This could modify not only contraction, with a possible participation in previously reported changes of contractility associated to aging [50,51], but also other Ca^{2+}-dependent functions. So, both mitochondrial activity and gene expression are likely targets for a long term modification of Ca^{2+} signal. We have recently shown in smooth muscle that even short-term exposures to elevated $[Ca^{2+}]_i$ modify the expression of important Ca^{2+}-handling proteins [52], therefore opening a possibility for progressive feed-back modification of Ca^{2+} signals. $[Ca^{2+}]_i$ transients induce an immediate modulation of the mitochondrial activity [53,54] and consequently a slowed decay can collaborate in the alterations of mitochondrial function observed during aging [3,42].

A practical consequence of our study is related to the effect of inhibitors in aged cells. The finding that inhibitors of Ca^{2+} extrusion mechanisms can accelerate the $[Ca^{2+}]_i$ decay in aged individuals poses potential side-effects in the therapeutic use of these types of compounds, as is the case for NCX inhibitors in some cardiovascular and renal diseases [55] because these

drugs could worsen the impairment of aged smooth muscle cells.

Acknowledgments

Pedro J. Gómez-Pinilla is recipient of a Ph.D. Fellowship of Junta de Extremadura (Spain). The study was supported by Spanish Ministry of Education (BFU 2004-0637) and Junta de Extremadura (2PR03A020).

REFERENCES

[1] Khachaturian ZS. Hypothesis on the regulation of cytosol calcium concentration and the aging brain. Neurobiol Aging 1987;8:345–6.
[2] Camello P, Gardner J, Petersen OH, Tepikin AV. Calcium dependence of calcium extrusion and calcium uptake in mouse pancreatic acinar cells. J Physiol 1996;490(Pt 3):585–93.
[3] Toescu EC, Verkhratsky A. Ca^{2+} and mitochondria as substrates for deficits in synaptic plasticity in normal brain ageing. J Cell Mol Med 2004;8:181–90.
[4] Toescu EC, Verkhratsky A. Parameters of calcium homeostasis in normal neuronal ageing. J Anat 2000;197(Pt 4):563–9.
[5] Kirischuk S, Voitenko N, Kostyuk P, Verkhratsky A. Age-associated changes of cytoplasmic calcium homeostasis in cerebellar granule neurons in situ: investigation on thin cerebellar slices. Exp Gerontol 1996;31:475–87.
[6] Martinez-Serrano A, Blanco P, Satrustegui J. Calcium binding to the cytosol and calcium extrusion mechanisms in intact synaptosomes and their alterations with aging. J Biol Chem 1992;267:4672–9.
[7] Smith DO. Cellular and molecular correlates of aging in the nervous system. Exp Gerontol 1988;23:399–412.
[8] Brewer GJ, Reichensperger JD, Brinton RD. Prevention of age-related dysregulation of calcium dynamics by estrogen in neurons. Neurobiol Aging 2006;27:306–17.
[9] Vanterpool CK, Vanterpool EA, Pearce WJ, Buchholz JN. Advancing age alters the expression of the ryanodine receptor 3 isoform in adult rat superior cervical ganglia. J Appl Physiol 2006;101:392–400.
[10] Gant JC, Sama MM, Landfield PW, Thibault O. Early and simultaneous emergence of multiple hippocampal biomarkers of aging is mediated by Ca^{2+}-induced Ca^{2+} release. J Neurosci 2006;26:3482–90.
[11] Vanterpool CK, Pearce WJ, Buchholz JN. Advancing age alters rapid and spontaneous refilling of caffeine-sensitive calcium stores in sympathetic superior cervical ganglion cells. J Appl Physiol 2005;99:963–71.
[12] Toescu EC, Verkhratsky A. Neuronal ageing from an intraneuronal perspective: roles of endoplasmic reticulum and mitochondria. Cell Calcium 2003;34:311–23.
[13] Howlett SE, Grandy SA, Ferrier GR. Calcium spark properties in ventricular myocytes are altered in aged mice. Am J Physiol Heart Circ Physiol 2006;290:H1566–74.
[14] Isenberg G, Borschke B, Rueckschloss U. Ca^{2+} transients of cardiomyocytes from senescent mice peak late and decay slowly. Cell Calcium 2003;34:271–80.
[15] Squier TC, Bigelow DJ. Protein oxidation and age-dependent alterations in calcium homeostasis. Front Biosci 2000;5:D504–26.
[16] Rubio C, Moreno A, Briones A, Ivorra MD, D'Ocon P, Vila E. Alterations by age of calcium handling in rat resistance arteries. J Cardiovasc Pharmacol 2002;40:832–40.
[17] Del CC, Ostrovskaya O, McAllister CE, Murray K, Hatton WJ, Gurney AM, et al. Effects of aging on Ca^{2+} signaling in murine mesenteric arterial smooth muscle cells. Mech Ageing Dev 2006;127:315–23.
[18] Maloney JA, Wheeler-Clark ES. Reduction in sarcoplasmic reticulum Ca^{2+}-ATPase activity contributes to age-related changes in the calcium content and relaxation rate of rabbit aortic smooth muscle. J Hypertens 1996;14:65–74.
[19] Lopes GS, Ferreira AT, Oshiro ME, Vladimirova I, Jurkiewicz NH, Jurkiewicz A, et al. Aging-related changes of intracellular Ca^{2+} stores and contractile response of intestinal smooth muscle. Exp Gerontol 2006;41:55–62.
[20] Xiong Z, Sperelakis N, Noffsinger A, Fenoglio-Preiser C. Changes in calcium channel current densities in rat colonic smooth muscle cells during development and aging. Am J Physiol 1993;265:C617–25.
[21] Szabo P, Weksler D, Whittington E, Weksler BB. The age-dependent proliferation of rat aortic smooth muscle cells is independent of differential splicing of PDGF A-chain mRNA. Mech Ageing Dev 1993;67:79–89.
[22] Yu HJ, Wein AJ, Levin RM. Age-related differential susceptibility to calcium channel blocker and low calcium medium in rat detrusor muscle: response to field stimulation. Neurourol Urodyn 1996;15:563–76.
[23] Gomez-Pinilla PJ, Camello-Almaraz C, Moreno R, Camello PJ, Pozo MJ. Melatonin treatment reverts age-related changes in Guinea pig gallbladder neuromuscular transmission and contractility. J Pharmacol Exp Ther 2006;319:847–56.
[24] Ishizuka J, Murakami M, Nichols GA, Cooper CW, Greeley Jr GH, Thompson JC. Age-related changes in gallbladder contractility and cytoplasmic Ca^{2+} concentration in the guinea pig. Am J Physiol 1993;264:G624–9.
[25] Geary GG, Buchholz JN. Selected contribution: effects of aging on cerebrovascular tone and $[Ca^{2+}]_i$. J Appl Physiol 2003;95:1746–54.
[26] Pagala MK, Tetsoti L, Nagpal D, Wise GJ. Aging effects on contractility of longitudinal and circular detrusor and trigone of rat bladder. J Urol 2001;166:721–7.
[27] Liu L, Ishida Y, Okunade G, Shull GE, Paul RJ. Role of plasma membrane Ca^{2+}-ATPase in contraction–relaxation processes of the bladder: evidence from PMCA gene-ablated mice. Am J Physiol Cell Physiol 2006;290: C1239–47.
[28] Wanaverbecq N, Marsh SJ, Al-Qatari M, Brown DA. The plasma membrane calcium-ATPase as a major mechanism for intracellular calcium regulation in neurones from the rat superior cervical ganglion. J Physiol 2003;550:83–101.
[29] Matsuda T, Arakawa N, Takuma K, Kishida Y, Kawasaki Y, Sakaue M, et al. SEA0400, a novel and selective inhibitor of the Na^+–Ca^{2+} exchanger, attenuates reperfusion injury in the in vitro and in vivo cerebral ischemic models. J Pharmacol Exp Ther 2001;298:249–56.
[30] Gibson JS, Muzyamba MC. Modulation of Gardos channel activity by oxidants and oxygen tension: effects of 1-chloro-2,4-dinitrobenzene and phenazine methosulphate. Bioelectrochemistry 2004;62:147–52.
[31] Orio P, Rojas P, Ferreira G, Latorre R. New disguises for an old channel: MaxiK channel beta-subunits. News Physiol Sci 2002;17:156–61.
[32] Imaizumi Y, Ohi Y, Yamamura H, Ohya S, Muraki K, Watanabe M. Ca^{2+} spark as a regulator of ion channel activity. Jpn J Pharmacol 1999;80:1–8.
[33] Liang W, Buluc M, van BC, Wang X. Vectorial Ca^{2+} release via ryanodine receptors contributes to Ca^{2+} extrusion from freshly isolated rabbit aortic endothelial cells. Cell Calcium 2004;36:431–43.
[34] Poburko D, Kuo KH, Dai J, Lee CH, van BC. Organellar junctions promote targeted Ca^{2+} signaling in smooth

muscle: why two membranes are better than one. Trends Pharmacol Sci 2004;25:8–15.
[35] van Breemen C, Lukeman S, Leijten P, Yamamoto H, Loutzenhiser R. The role of superficial SR in modulating force development induced by Ca entry into arterial smooth muscle. J Cardiovasc Pharmacol 1986;8(Suppl. 8):S111–6.
[36] Daniel EE, El-Yazbi A, Cho WJ. Caveolae and calcium handling, a review and a hypothesis. J Cell Mol Med 2006;10:529–44.
[37] Moore ED, Voigt T, Kobayashi YM, Isenberg G, Fay FS, Gallitelli MF, et al. Organization of Ca^{2+} release units in excitable smooth muscle of the guinea-pig urinary bladder. Biophys J 2004;87:1836–47.
[38] Yoshikawa A, van Breemen C, Isenberg G. Buffering of plasmalemmal Ca^{2+} current by sarcoplasmic reticulum of guinea pig urinary bladder myocytes. Am J Physiol 1996;271:C833–41.
[39] Duchen MR. Mitochondria and calcium: from cell signalling to cell death. J Physiol 2000;529(Pt 1):57–68.
[40] Murchison D, Griffith WH. Increased calcium buffering in basal forebrain neurons during aging. J Neurophysiol 1998;80:350–64.
[41] Pottorf WJ, Duckles SP, Buchholz JN. Adrenergic nerves compensate for a decline in calcium buffering during ageing. J Auton Pharmacol 2000;20:1–13.
[42] Xiong J, Camello PJ, Verkhratsky A, Toescu EC. Mitochondrial polarisation status and $[Ca^{2+}]_i$ signalling in rat cerebellar granule neurones aged in vitro. Neurobiol Aging 2004;25:349–59.
[43] Lin AT, Hsu TH, Yang C, Chang LS. Effects of aging on mitochondrial enzyme activity of rat urinary bladder. Urol Int 2000;65:144–7.
[44] Morgan AJ, Jacob R. Differential modulation of the phases of a Ca^{2+} spike by the store Ca^{2+}-ATPase in human umbilical vein endothelial cells. J Physiol 1998;513(Pt 1):83–101.
[45] Camello C, Pariente JA, Salido GM, Camello PJ. Role of proton gradients and vacuola H(+)-ATPases in the refilling of intracellular calcium stores in exocrine cells. Curr Biol 2000;10:161–4.
[46] Wu C, Fry CH. $Na(^{+})/Ca(^{2+})$ exchange and its role in intracellular $Ca(^{2+})$ regulation in guinea pig detrusor smooth muscle. Am J Physiol Cell Physiol 2001;280: C1090–6.
[47] Lee C, Visen NS, Dhalla NS, Le HD, Isaac M, Choptiany P, et al. Inhibitory profile of SEA0400 [2-[4-[(2,5-difluorophenyl)methoxy]phenoxy]-5-ethoxyaniline] assessed on the cardiac Na^{+}–$Ca2^{+}$ exchanger, NCX1.1. J Pharmacol Exp Ther 2004;311:748–57.
[48] Ren X, Kasir J, Rahamimoff H. The transport activity of the Na^{+}–Ca^{2+} exchanger NCX1 expressed in HEK 293 cells is sensitive to covalent modification of intracellular cysteine residues by sulfhydryl reagents. J Biol Chem 2001;276: 9572–9.
[49] Iwamoto T, Kita S, Uehara A, Imanaga I, Matsuda T, Baba A, et al. Molecular determinants of Na^{+}/Ca^{2+} exchange (NCX1) inhibition by SEA0400. J Biol Chem 2004;279:7544–53.
[50] Andersson KE, Arner A. Urinary bladder contraction and relaxation: physiology and pathophysiology. Physiol Rev 2004;84:935–86.
[51] Nordling J. The aging bladder—a significant but underestimated role in the development of lower urinary tract symptoms. Exp Gerontol 2002;37:991–9.
[52] Morales S, Diez A, Puyet A, Camello P, Camello-Almaraz C, Bautista J, et al. Calcium controls smooth muscle TRPC gene transcription via the CAMK/calcineurin-dependent pathways. Am J Physiol Cell Physiol 2006.
[53] Voronina S, Sukhomlin T, Johnson PR, Erdemli G, Petersen OH, Tepikin A. Correlation of NADH and Ca^{2+} signals in mouse pancreatic acinar cells. J Physiol 2002;539:41–52.
[54] Hajnoczky G, Robb-Gaspers LD, Seitz MB, Thomas AP. Decoding of cytosolic calcium oscillations in the mitochondria. Cell 1995;82:415–24.
[55] Iwamoto T, Kita S. Development and application of Na^{+}/Ca^{2+} exchange inhibitors. Mol Cell Biochem 2004;259: 157–61.